Clarke, D., MacDonald, E.C. and Owens, S. (2004) *Li abundance/surface activity connections in solar-type Pleiades.* Astronomy and Astrophysics, 415 (2). pp. 677-684. ISSN 0004-6361

http://eprints.gla.ac.uk/28165/

Deposited on: 14 February 2012

A&A 415, 677–684 (2004)
DOI: 10.1051/0004-6361:20034620

Astronomy & Astrophysics

Li abundance/surface activity connections in solar-type Pleiades

D. Clarke[1], E. C. MacDonald[2], and S. Owens[1]

[1] Department of Physics and Astronomy, University of Glasgow, Glasgow G12 8QQ, Scotland, UK
[2] Department of Astrophysics, University of Oxford, Denys Wilkinson Building, Keble Road, Oxford OX1 3RH, UK

Received 14 April 2003 / Accepted 13 November 2003

Abstract. The relation between the lithium abundance, $A_{\rm Li}$, and photospheric activity of solar-type Pleiads is investigated for the first time via acquisition and analysis of B and V-band data. Predictions of activity levels of target stars were made according to the $A_{\rm Li}/(B-V)$ relation and then compared with new CCD photometric measurements. Six sources behaved according to the predictions while one star (HII 676), with low predicted activity, exhibited the largest variability of the study; another star (HII 3197), with high predicted activity, was surprisingly quiet. Two stars displayed non-periodic fadings, this being symptomatic of orbiting disk-like structures with irregular density distributions. Although the observation windows were not ideal for rotational period detection, some periodograms provided possible values; the light-curve obtained for HII 1532 is consistent with that previously recorded.

Key words. stars: solar-type – stars: rotation

1. Introduction

The observational study by Duncan & Jones (1983) of G & K type stars in the Pleiades indicated a much larger dispersion of surface lithium abundance, $A_{\rm Li}$ [$= 12 + \log\{N({\rm Li})/N({\rm H})\}$], than expected for a cluster of its age (∼75/100 Myrs). An early explanation suggested that the members form an age dispersion (Duncan & Jones 1983; Butler et al. 1987) but this notion has since been abandoned. Subsequent studies by Soderblom et al. (1993a) and Jones et al. (1996) confirmed the $A_{\rm Li}$ dispersion, being most pronounced for stars with $M < 0.9\,M_{\odot}$. They claimed that rapid rotators (high $v \sin i$) have preserved more of their initial Li relative to slow rotators of similar mass. Some fast rotators appear to have preserved all their initial Li. According to Jones et al. (1996), the association of high $v \sin i$ with undepleted $A_{\rm Li}$ results from rapid rotation affecting the circulation current sufficiently to prevent Li accumulating near the bases of the convective zones where the temperature is sufficient for Li to be destroyed. The observational studies of Soderblom et al. (1993a) and Jones et al. (1996) also showed that stars with low Li-depletion have a tendency to display chromospheric activity, although this alone was unable to account for the $A_{\rm Li}$ dispersion.

Concurrently, Soderblom et al. (1993b) demonstrated that chromospheric activity, based on emission measures of Hα and Ca II 8542 Å, was correlated with rotation after normalising $v \sin i$ values to a parameter akin to the Rossby number of each star. Many stars display temporal variability in the chromospheric lines, degrading the correlation, based as it is on synoptic measurements. The question of the dispersion of $A_{\rm Li}$ at a given stellar mass being related to temporal variability in the Li I 6708 Å line has, been ruled out, however, by Jeffries (1999).

In pursuit of understanding the reasons for the $A_{\rm Li}$ dispersion, King et al. (2000) have re-examined many of the complex issues of the Li/rotation connection in more comprehensive ways. They have presented evidence that dispersion in equivalent widths of the Li line is caused by stellar atmospheric effects rather than being wholly related to genuine abundance differences. Using more rigorous statistical methods than in previous studies, they have confirmed a strong correlation between stellar activity and Li-excess but not a one-to-one perfect mapping between $A_{\rm Li}$ and stellar rotation, based on determined periods rather than $v \sin i$ projections.

All the discussions within the papers cited above bear testament to the very complex issues relating the various observed parameters and to the problems addressed to explain the range of $A_{\rm Li}$ in coeval stars, this being key to our understanding of early stellar evolutionary processes and of their time scales.

Recently, Messina et al. (2001) have investigated the "rotation-photospheric activity connection" using the diagnostics of V-band light-curve amplitudes as being indicators of starspot coverage and magnetic activity. From a compilation of various data they have found a high degree of correlation between the envelope of maximum V-band light-curve amplitudes and the rotation period in five open clusters, including the Pleiades. In this paper the relationship between $A_{\rm Li}$ and *photospheric* activity is explored for the first time by assessing data from the literature and by new measurements presented here.

Send offprint requests to: D. Clarke,
e-mail: d.clarke@astro.gla.ac.uk

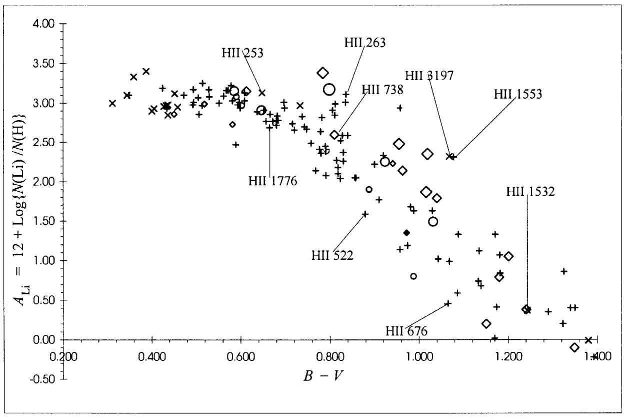

Fig. 1. The $(B-V)/A_{\rm Li}$ diagram for the Pleiades with 27 stars, monitored previously for photospheric activity, highlighted. For fast rotators ($v \sin i > 30\,{\rm km\,s^{-1}}$), diamond symbols [$\diamond \longrightarrow \Diamond$] indicate the degree of activity by their size; for slow rotators ($v \sin i < 30\,{\rm km\,s^{-1}}$), increasing sizes of circle [$\circ \longrightarrow$ O] indicate the degree of activity. The 8 target stars are indicated by their HzC number. Another marked star, HII 738, in the same field of a target and previously measured for activity, was also monitored. Other stars are simply marked according to their rotation being rapid ("×") or slow ("+").

Figure 1 provides the $(B-V)/A_{\rm Li}$ diagram for the Pleiades with additional information on photospheric activity and rotation. The basic positions of each star were obtained from Jones et al. (1996) and Soderblom et al. (1993a). Activity estimates were obtained from broad-band photometry for 27 stars from van Leeuwen & Alphenaar (1982), Panov & Geyer (1991), Magnitskii (1987a,b), Stauffer & Hartmann (1987) and O'Dell et al. (1995); the estimates are on a sliding scale with high activity set at $\gtrsim 0\overset{\rm m}{.}25$, medium activity $\sim 0\overset{\rm m}{.}1$, and low activity being just above detectable limits ($\sim 0\overset{\rm m}{.}01$). These activity estimates have been combined with rotational velocity data from Stauffer & Hartmann (1987). Inspection of Fig. 3 in Stauffer et al. (1984), suggests a bimodal distribution of rotational velocities with fast rotators being in a group with $v \sin i \gtrsim 30\,{\rm km\,s^{-1}}$; stars with $v \sin i > 30\,{\rm km\,s^{-1}}$ have been classed as ultra-fast rotators (UFRs) by Soderblom et al. (1993b).

The stars with estimated activities are plotted for UFRs, with increasing sizes of diamond [$\diamond \longrightarrow \Diamond$], according to the amplitude of activity; for slow rotators ($v \sin i < 30\,{\rm km\,s^{-1}}$), the degree of activity is noted by increasing sizes of circle [$\circ \longrightarrow$ O]. Stars of unknown activity are simply marked as "+" or "×" according to whether they are slow or rapid rotators respectively. The spread in $A_{\rm Li}$ is clear for stars of $(B-V) > 0.7$ (late G- to K-type). For stars of a given colour, the dispersion reveals a tendency for the more photospheric active stars to have higher $A_{\rm Li}$. The same tendency related to fast rotators, referred to earlier, can also be seen.

In order to extend the data base for degree of variability of stars with measured $A_{\rm Li}$ and to gain better understanding of the $A_{\rm Li}$/activity tendency, 8 stars marked in Fig. 1 by catalogue number (Hertzsprung 1947, later referred to as HzC) were observed with the JKT in La Palma using the CCD imager (TEK4 detector); some 40 other stars within the target fields were investigated. Data for B and V filters were obtained during November 1998, the 7 consecutive nights having Julian Dates running from 245 1141.3 to 245 1147.7, each night simply being referred to as JD 41 to JD 47 inclusively. From the suggested tendency highlighted above, the activities of the 8 targets were predicted according to their position in the $(B-V)/A_{\rm Li}$ diagram, with details given in Table 1, towards the end of the paper; B and $(B-V)$ are taken from photoelectric measurements of Johnson & Mitchell (1958, later referred to as J&M). The major aim of the exercise was to compare these predicted activity estimates with the new photometric observations.

2. Data reduction and analysis techniques

The targets were positioned in the frame to allow acquisition of a selection of field stars required for differential photometry. Where possible, B and V frames for each target were taken as sequence pairs with exposures from 10 s to 120 s according to the brightness of the target and the seeing quality. Dark, bias and twilight flat-field frames were obtained as standard procedure. Data reduction was performed using the Starlink package CCDPACK. Once the frames were flat-fielded, bias subtracted and aligned, the package AUTOPHOTOM was implemented to extract magnitudes for the monitored stars. This reduction gives error estimates based on the variance component of the data array which, for most frames, gave determinations correct to $\sim\pm 0\overset{\rm m}{.}001$, with differential photometry achieved to an accuracy of a few milli-mags.

Although each field contained at least one star with B, V values from J&M, no true standards were observed. Without a full transformation procedure, the values reported here are essentially "instrumental" and designated B_i, V_i, although any differences from their underlying standard B, V values are likely to be very small. In considering the results, it must be remembered that the B, V reference values of J&M are synoptic and may carry systematic errors since these stars are variable. Further small systematic errors may also be present in the mean B_i, V_i of each field star resulting from their own possible variability. In assessing the variability of each monitored star, a problem arises from not knowing which field star can be taken as a stable reference. Since the stars have similar brightness, they are likely to be of similar spectral type and are all probably variable to some degree.

Firstly, the problem was tackled by taking each star in turn to act as reference, so providing magnitude differences designated by ΔB_i, ΔV_i, according to the passband. Assessment of activity was made by inspection of these values simply plotted as time sequences. An example from such an exercise is given in Fig. 2. Inter-comparison of all the various temporal patterns of ΔB_i, ΔV_i provided insight on the activity of each star. If, for example, relative to a particular reference star, the temporal variations ΔB_i, ΔV_i for all the other stars displayed the same signatures, this indicated variability of the reference object itself. Selection of the best comparison stars was made by considering magnitude differences which were not mirrored from one star to the next, or which for some star pairs, showed no statistically significant variations at all.

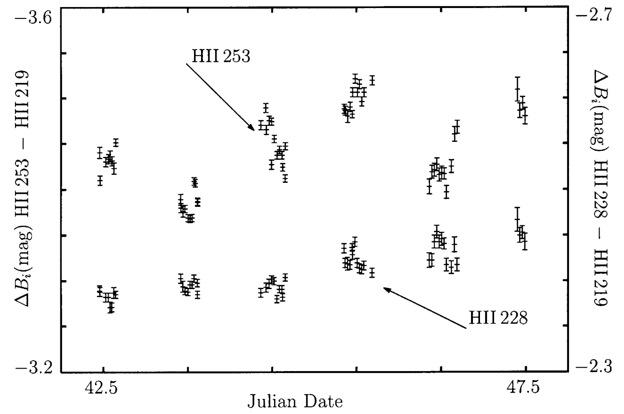

Fig. 2. Using HII 229 as the reference star, ΔB_i values for HII 253 show night-to-night variations, with drifting changes on each night particularly well seen around JD 44, at the phase of the light-curve mid-point when the changes are at their fastest. For HII 228 there is a steady rise in brightness over the 6 nights, probably related to a longer period of variability.

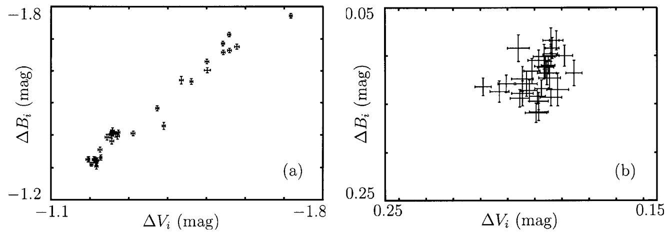

Fig. 3. a) Contemporaneous $\Delta B_i, \Delta V_i$ magnitude differences of HII 676 – HII 655 are displayed, indicating a large variability of the target star over a range $\sim 0\overset{\mathrm{m}}{.}5$. **b)** The $\Delta B_i, \Delta V_i$ behaviour of HII 711 – HII 655 suggests that neither star displays any significant variability greater than the noise $\sim \pm 0\overset{\mathrm{m}}{.}01$.

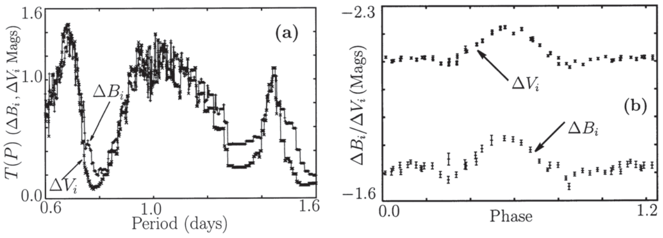

Fig. 4. a) The LK periodograms based on $\Delta B_i, \Delta V_i$ for HII 1532 – HII 1575 provide a minimum at $0\overset{\mathrm{d}}{.}777$. **b)** The $\Delta B_i, \Delta V_i$ values phased on a period of $0\overset{\mathrm{d}}{.}777$ show the outlines of the underlying coherent light-curves.

Secondly, for those occasions when B, V frames were exposed in quick succession, the contemporaneous differences, $\Delta B_i, \Delta V_i$, may be plotted against each other. According to van Leeuwen et al. (1987), periodic variable solar-type Pleiads display only marginal colour index changes. B and V-band variations are therefore correlated, and display a linear relationship. If the disturbing features, with small temperature differences relative to the undisturbed photosphere, traverse the projected disk, the change in B is slightly greater than for V and hence the B/V gradient should be just greater than unity; this is independent of whether the features are bright patches or dark spots. The determined gradient is independent of any interstellar extinction affecting the star's colour. Whether or not stars are active can therefore be checked by investigating the correlation between the $\Delta B_i, \Delta V_i$ values. As the measurements were made under fairly constant conditions, with very similar error values for the differential magnitude determinations, the required $\Delta B_i/\Delta V_i$ and $\Delta V_i/\Delta B_i$ gradients for the exercise were calculated without weighting of the individual measurements, with a correlation coefficient determined by the standard method. Following any marked correlation, the degree of activity was estimated from the spread of the ΔV_i values in the $\Delta B_i, \Delta V_i$ plot. For data with a low level of correlation but with dispersions of $\Delta B_i, \Delta V_i$ larger than that associated with measurement noise, both stars may be considered as being variable. For star pairs with little or no activity, the $\Delta B_i, \Delta V_i$ values overlap within a spread of their joint distribution according to the measurement uncertainties.

Two examples of the behaviour of contemporaneous $\Delta B_i, \Delta V_i$ measurements are given in Fig. 3, one displaying strong activity of either the target star or its reference, the other showing little or no variation of the two compared stars to the limit of the measurement noise.

The data distribution in the $\Delta B_i, \Delta V_i$ plane may also provide insight on the variability. If a star is measured at random and has a sinusoidal-like variation, the values will be located according to the principles of simple harmonic motion, with more measurements likely to be made at the light-curve maxima and minima, where the rates of change are slowest. The density of points will tend to concentrate at the extremes of the linear distribution rather than at mid-level values; such behaviour shows in Fig. 3a.

Thirdly, the data were subjected to string/rope analysis, providing periodograms from the regularised Lafler-Kinman (LK) statistic, $T(P)$, (see Clarke 2002: Eq. (3)). Periodograms were investigated for the B and V-bands separately and their combination. As several stars were monitored in each recorded frame, those stars deemed to be stable were used to explore sampling and windowing effects. Because of the relatively short time span of this photometric exercise, it was not expected that periods would be determinable for most of the monitored stars. A good example of the behaviour of an LK periodogram and a resulting light-curve are provided in Fig. 4 for HII 1532.

The three analysis schemes outlined above were applied to each of the 8 selected fields. The monitored stars are identified in Table 1 with their determined values of B_i, V_i and $(B_i - V_i)$.

3. The results

3.1. Field 1: HII 253

Summary: B-band 60 frames; V-band 50 frames;
Six nights of observation from JD 42 to JD 47;
J&M lists only HII 263 for reference B, V values;
Six field stars monitored with HzC identification;
HII 219 was taken as the stable, reference object.

The temporal behaviour of HII 253 (see Fig. 2) gives evidence of an underlying period. On JD 44, the brightness displayed a progressive drop possibly at the falling mid-point of a

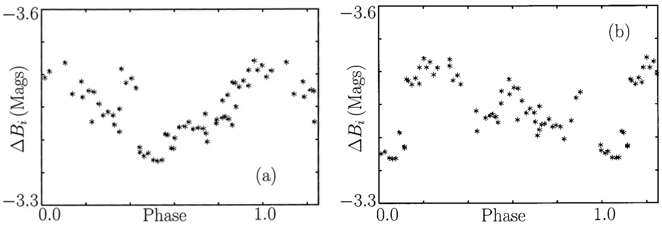

Fig. 5. a) Phased on a period of $1\overset{\mathrm{d}}{.}365$ the ΔB_i for HII 253 – HII 219 provides a sketched near-sinusoidal light-curve but with spike. **b)** The same data phased on a period of $1\overset{\mathrm{d}}{.}717$ provides the outline of a less distinctive light-curve.

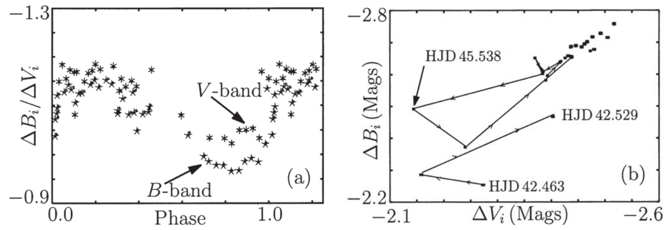

Fig. 6. a) The ΔB_i, ΔV_i differences for HII 263 – HII 257 phased on a period of $0\overset{\mathrm{d}}{.}848$ show a rudimentary light-curve, the two-colour variations being in phase. **b)** The ΔB_i, ΔV_i correlation of HII 282 – HII 257 shows fading of HII 282 ~ $0\overset{\mathrm{m}}{.}3$ on JD 42 and JD 45; on the latter night, the star faded and recovered, the episode covering ~$3\overset{\mathrm{h}}{.}2$.

light-curve when the changes are at their fastest. The range of the variation is ~$0\overset{\mathrm{m}}{.}2$. The lower portion of Fig. 2 reveals HII 228 to be variable, with a smaller range (~$0\overset{\mathrm{m}}{.}08$) and with a period longer than 7 days.

The ΔB_i, ΔV_i plot based on HII 253 – HII 219 confirmed the target's variability with data density enhancement at minimum brightness, suggesting the sampling of a sinusoidal-like light-curve. The paucity of measurements at higher brightness suggest the observation windows do not cover the light maximum. Although ΔV_i had a range ~$0\overset{\mathrm{m}}{.}16$, the true span is probably greater, perhaps ~$0\overset{\mathrm{m}}{.}2$, giving a light-curve amplitude ~$0\overset{\mathrm{m}}{.}1$. The determined $\Delta B_i/\Delta V_i$ gradient was 1.06, a value in keeping with disturbed patches on the stellar surface with temperatures differing by a few hundred degrees from the mean photosphere, the same cells also causing the brightness changes.

The periodogram for ΔB_i gave minima at $1\overset{\mathrm{d}}{.}365$ and $1\overset{\mathrm{d}}{.}717$. The former period provides a near sinusoidal light-curve but with a sharp departure over a phase interval ~0.1 (see Fig. 5a). This "spike" relates to data recorded on the last night. It also occurs in the V-band light-curve and is likely caused by a rapid change in the disposition of the surface features rather than by flare activity. Marilli et al. (1997) have reported a period of $1\overset{\mathrm{d}}{.}721$. If the data are phased on the suggested close value of $1\overset{\mathrm{d}}{.}717$, the ensuing light-curve (Fig. 5b) shows a more complicated structure. Further observations are required to confirm the period of this star.

HII 272 was variable with changes of ~$0\overset{\mathrm{m}}{.}05$ but with a weak correlation between the B and V measurements, the result perhaps being influenced by possible small scale variability of the reference star, HII 219. The data for both HII 203 and HII 217, set variation limits of ~$0\overset{\mathrm{m}}{.}01$. However, the important outcome of this exercise is the scale of the light variations of HII 253, confirming the medium/high level activity prediction in Table 1.

Being redder than other field stars and with brightnesses just above the main sequence trend (see Fig. 9), HII 217 and HII 272 are candidates for possessing unresolved companions. The population of such solar-type photometric binaries within the Pleiades is estimated at 26% by Stauffer (1984).

3.2. Field 2: HII 263

Summary: B-band 41 frames; V-band 34 frames;
Six nights of observation;
J&M lists only HII 263 for reference B, V values;
Five field stars with HzC identification;
HII 257 displayed least activity – used as stable reference;
HII 282 showed discrepant brightness compared with HzC.
The ΔB_i, ΔV_i values were strongly correlated with a gradient of 1.16 and with ΔV_i varying by ~$0\overset{\mathrm{m}}{.}18$, validating the prediction for HII 263 in Table 1.

A suggested period of $0\overset{\mathrm{d}}{.}851$ produced in-phase rudimentary light-curves for the two colours (see Fig. 6a). Based on HII 263 – HII 322 and HII 263 – HII 309, periods of $0\overset{\mathrm{d}}{.}859$ and $0\overset{\mathrm{d}}{.}848$ also emerged. According to Krishnamurthi et al. (1998), HII 263 has a period of $4\overset{\mathrm{d}}{.}82$; folding the data on this covered only three quarters of the cycle but with fluctuations, suggesting a poor fit. A longer data run and a further investigation of reference stars are required to confirm the correct period.

HII 282 displayed a peculiar behaviour. For most of the run, $\Delta B_i/\Delta V_i$ data gave a strong correlation with a gradient of 1.17, similar to the behaviour of other spotted rotating stars. On the night of JD 45, however, the star faded with a fall ~$0\overset{\mathrm{m}}{.}3$ before recovering, the episode covering ~$3\overset{\mathrm{h}}{.}2$ (see Fig. 6b). The three measurements on JD 42 also provide anomalous low brightness values. As such behaviour was unexpected, particular checks were made on these data frames. There was no evidence of poor image registrations; the anomalies only affected HII 282 and, as it was fairly central to the field, no technical reason was apparent to explain the behaviour. Its m_{pg} value in HzC differs by ~5 mags from the mean B_i determined here. Thus the HzC value may have been obtained either at a time of extreme low brightness or there is a misprint in the catalogue. Its position relative to the main sequence trend (see Fig. 9) and its red colour with respect to the other field stars make it a possible photometric binary candidate, raising a question of the system being a short-period eclipsing binary involving a faint red dwarf. The behaviour of the events are more akin, however, to the non-periodic Algol-type minima associated with HAEBE objects, with UX Ori as prototype (Bibo & Thé 1991). For these young objects, the photometric behaviour is modelled in terms of irregular dust flows within disk-like envelopes, producing variable scattering and extinction (see, for example, Rostopchina et al. 1997). HII 282 certainly deserves a more intensive photometric investigation.

The ΔB_i, ΔV_i values for HII 322 – HII 257 also indicate a strong variability of HII 322 with range ΔV_i ~ $0\overset{\mathrm{m}}{.}16$. Slightly larger variability was noted for HII 309 with ΔV_i ~ $0\overset{\mathrm{m}}{.}18$. Periodograms for HII 322 and HII 309 both displayed similar

Table 1. The monitored stars in 8 fields are tabulated with their mean B_i magnitudes and colour values, $B_i - V_i$. At the head of each block, the target star is noted with indication of its rotation speed ([F]ast or [S]low) and its activity prediction (1 = high, 2 = medium and 3 = low). The star taken as the field magnitude reference is also given, its B_i and $B_i - V_i$ values corresponding to B and $B - V$ in J&M. Under "Var V_i" estimates are noted of the total V_i variation due to photospheric features. The co-ordinates ascribed to the non-cataloged stars listed in the bottom left hand section are for Epoch 2000.0 and are estimates based on the other stars in the field and on the plate scale.

HII	m_{pg}	A_{Li}	B_i	$B_i - V_i$	Var V_i	Comments
Field 1			**HII 253 [F: 2/1]**		**Ref: HII 253**	
203	15.13	—	15.26	+0.72	$<0^{\rm m}.01$	—
217	13.11	—	12.90	+1.07	$<0^{\rm m}.01$	—
219	14.71	—	14.78	+0.74	—	—
223	16.1	—	16.37	+0.80	—	—
228	12.57	—	12.38	+0.61	$0^{\rm m}.08$	—
253	11.30	3.13	11.34	+0.68	$0^{\rm m}.20$	$P = 1^{\rm d}.365$
272	14.31	—	14.09	+1.70	$0^{\rm m}.05$	Very red
Field 2			**HII 263 [S: 1]**		**Ref: HII 263**	
225	13.97	—	14.34	+0.73	—	—
257	13.30	—	13.50	+0.84	—	—
263	12.30	3.11	12.42	+0.88	$0^{\rm m}.18$	$P = 0^{\rm d}.851$
282	15.90	—	10.93	+0.64	$0^{\rm m}.05$	Peculiar
309	11.27	—	11.37	+0.71	$0^{\rm m}.18$	—
322	12.58	—	12.72	+0.77	$0^{\rm m}.16$	—
Field 3			**HII 522 [S: 3]**		**Ref: HII 522**	
522	12.80	1.59	12.87	+0.94	$0^{\rm m}.10$	Peculiar
575	14.93	—	15.26	+1.18	—	—
598	15.88	—	16.86	+1.16	—	—
616	15.35	—	15.88	+1.25	—	—
Field 4			**HII 676 [S: 3]**		**Ref: HII 738 [F: 1/2]**	
625	13.71	—	13.80	+1.16	$0^{\rm m}.50$	—
655	15.82	—	16.28	+1.23	—	—
676	14.59	0.46	14.72	+1.26	$0^{\rm m}.50$	—
711	16.0	—	16.46	+1.15	—	—
738	13.42	2.60	13.42	+1.16	$0^{\rm m}.15$	—

Non-Catalogued Stars:			
		#4:	03 48 25.7 +25 12 35
#1:	03 47 34.1 +23 45 06	#5:	03 48 18.7 +25 12 35
#2:	03 47 39.2 +22 56 43	#6:	03 52 11.7 +24 38 13
#3:	03 47 43.4 +22 57 07	#7:	03 52 06.6 +24 38 42

HII	m_{pg}	A_{Li}	B_i	$B_i - V_i$	Var V_i	Comments
Field 5			**HII 1532 [S: 3/2]**		**Ref: HII 1532**	
1427	14.70	—	15.05	+1.22	—	—
1457	15.41	—	15.90	+0.66	—	—
#1	—	—	17.57	+0.79	—	—
1478	15.92	—	16.51	+1.05	—	—
1493	16.2	—	16.41	+0.63	—	—
1532	14.92	0.37	15.21	+1.26	$0^{\rm m}.15$	$P = 0^{\rm d}.777^*$
1534	16.4	—	16.79	+0.80	—	—
1545	15.39	—	15.81	+0.72	—	—
1570	14.89	—	15.13	+1.08	—	—
1575	16.6	—	16.94	+0.87	—	—
1582	15.42	—	15.66	+1.27	$0^{\rm m}.05$	—
Field 6			**HII 1553 [S: 1]**		**Ref: HII 1553**	
1508	14.14	—	14.13	+0.71	—	—
#2	—	—	15.25	+0.54	—	—
1553	13.25	2.31	13.28	+1.06	$0^{\rm m}.07$	—
1554	12.56	—	12.49	+0.66	—	—
#3	—	—	15.99	+0.74	—	
Field 7			**HII 1776 [S: 2/3]**		**Ref: HII 1776**	
1776	11.60	2.72	11.63	+0.72	$0^{\rm m}.05$	—
#4	—	—	17.05	+0.98	—	—
#5	—	—	16.87	+1.11	—	—
1844	12.29	—	11.53	+0.32	$0^{\rm m}.07$	—
1900	11.43	—	12.22	+1.21	—	—
Field 8			**HII 3197 [F: 1]**		**Ref: HII 3197**	
3167	14.23	—	14.80	+0.68	$0^{\rm m}.25$	$P = 0^{\rm d}.901$
3197	13.06	2.32	13.36	+1.10	$<0^{\rm m}.03$	Very quiet
3198	14.89	—	15.31	+0.78	$0^{\rm m}.08$	
#6	—	—	16.42	+0.85	—	—
#7	—	—	16.48	+0.84	—	—

structures likely caused by sampling and windowing effects and no periods could be assigned.

3.3. Field 3: HII 522

Summary: B-band 47 frames; V-band 38 frames;
J&M lists only HII 522 for reference B, V values;
Number of nights monitored: 6;
3 field stars monitored with HzC identification;
HII 575 displayed least activity – used as stable reference.
The activity of the monitored stars was noticeably less than for the two previously discussed fields. HII 522 was the most active star. Intercomparison of the various time plots revealed brightness changes on the nights of JD 45 and JD 46; on other nights any variability was marginal. No periodicities were detectable in any of the stars.

The ΔB_i, ΔV_i plots of HII 522 showed most values contained within a small area appropriate to the measurement uncertainties, indicating low activity. Between HJD 46.483 to 46.696 it became $\sim 0^{\rm m}.1$ fainter, however, but with no significant colour change. This signature could not be ascribed to any photometric technical problem. Its position relative to the main sequence trend (see Fig. 9) makes it a photometric binary candidate. The fading behaviour was similar to HII 282 and again might be ascribed either to the star being a short-period eclipsing binary or to irregular orbiting dust clouds imposing their effects on a small rotational modulation of active photospheric areas, the scale of the latter supporting the prediction of Table 1.

It may be noted also that on the nights JD 41 to JD 43 no variations between HII 575 and HII 598 were detectable, as also for the nights JD 44 to JD 47. If the two time sections are averaged, however, HII 598 increased in brightness by $\sim 0^{\rm m}.05$ relative to HII 575.

All the colour values are larger than expected, typically by $0^{\rm m}.3$. A polarimetric study by Breger (1986) revealed that this cluster area is affected by interstellar material. One of the field stars, HII 575, classed as a cluster non-member, displays $p = 0.93\%$, a value sufficiently high to account for its apparent colour excess.

3.4. Field 4: HII 676

Summary: B-band 33 frames; V-band 34 frames;
Observations on nights JD 44, JD 45, and JD 46 only;

4 field stars monitored with HzC identification;
J&M lists HII 625, HII 676 and HII 738 with B, V values;
HII 738 used as the magnitude reference;
HII 655 displayed least activity – used as stable reference.
Although noted by Krishnamurthi et al. (1998) as periodic, HII 738 exhibited smaller activity than HII 625 and HII 676 and was used as reference to provide mean B_i, V_i magnitudes for the other stars. Comparison with J&M shows HII 625 to be fainter by $0^m_.09$ and $0^m_.07$ in B_i and V_i respectively, while HII 676 is brighter by $0^m_.14$ and $0^m_.21$ for the two bands. Such differences highlight the earlier discussed problems of assigning magnitudes in this exercise.

The $\Delta B_i, \Delta V_i$ plot for HII 711 – HII 655 (see Fig. 3b) shows neither star exhibiting variability; the tightly distributed data have dispersion according to the measurement noise ($\sim\pm 0^m_.007$). Using HII 655 as reference, the target star (HII 676) and HII 625 both displayed high activity $\sim 0^m_.5$. With respect to the prediction, HII 676 is more active than expected.

HII 738 shows ΔV_i to vary by $\sim 0^m_.15$. Listed in Soderblom et al. (1993a), with an $A_{\rm Li}$ value of 2.6, it would be expected to display medium to high activity, the measurements here agreeing with the prediction.

From three nights only, period detections were not anticipated. Alternative periods for HII 738 are noted in the literature: Krishnamurthi et al. (1998) give $0^d_.83$ while Marilli et al. (1997) give $1^d_.460$. This discrepancy could not be resolved by the limited data here. Although the periodogram for HII 625 suggested a period of $0^d_.466$, close to the values of $0^d_.422$, determined by Magnitskii (1987a) and $0^d_.428$ by van Leeuwen et al. (1987), the LK minimum was not statistically significant. More extensive photometry is certainly required for this field.

All the stars have larger colour values than expected with excesses just greater than $0^m_.3$. Breger (1986) showed this area to display high interstellar polarization and significant reddening. Stauffer & Hartmann (1987) give reddening estimates of 0.34, 0.28 and 0.40 for HII 625, HII 676 and HII 738 respectively. It may be noted that HII 738 has been found by Bouvier et al. (1997) to have a companion separated by $0''_.50$ and this may affect the perceived colour.

3.5. Field 5: HII 1532

Summary: B-band 38 frames; V-band 37 frames;
Observations on 4 nights JD 44 to JD 47;
J&M lists only HII 1532 with B, V values;
10 field stars monitored, 9 with HzC identification;
HII 1575 used as stable reference.
HII 1532 was markedly the most variable in the field. Periods from $0^d_.771$ to $0^d_.795$ were obtained, according to the chosen reference star. Based on $\Delta B_i, \Delta V_i$, joint periodograms from HII 1532 – H II 1575 gave $0^d_.777$ with coherent light-curves for the two bands as depicted in Fig. 4b. Krishnamurthi et al. (1998) reported a period of $0^d_.78$, with variation of similar form. A brightness enhancement, covering about half of the period, suggests the presence of a single feature traversing the projected stellar disk and being obscured during the other half of the cycle. The range of the variation of V_i was $\sim 0^m_.15$, in keeping with the Table 1 prediction.

HII 1582 displayed small activity. Its periodogram suggested a period $\sim 0^d_.95$ but the engendered light-curves had inadequate phase coverage, being based on only four consecutive nights of observation. The variability was small, $\sim 0^m_.05$ in the V-band. Little or no variability was detected for the other field stars.

Four of the listed stars in Table 1 have colour values $>1^m_.0$ suggesting that they suffer from reddening. Whether this results from interstellar material or more localised dust might perhaps be resolved by further photometric studies using a larger range of wavebands or by polarimetric studies. The field is towards the cluster edge and was beyond the areas covered by Breger's (1986) polarimetric study and was not included in the reddening estimates of Stauffer & Hartmann (1987).

3.6. Field 6: HII 1553

Summary: B-band 28 frames; V-band 28 frames;
Observations on nights JD 42, JD 43, and JD 44 only;
J&M lists only HII 1553 with B, V values;
4 field stars monitored, 2 with HzC identification;
HII 1508 used as stable reference.
All the monitored stars appeared to be relatively inactive. Only HII 1553 provided a recognisable signature showing a maximum on JD 43 and a progressive fall on JD 44, suggesting a period of just less than one day. The sparse data produced periodograms with no statistically significant minima. The variation in ΔV_i was $\sim 0^m_.07$, this being a little below the prediction for HII 1553 in Table 1.

For the other four stars, all are variables of small amplitude. The $\Delta B_i, \Delta V_i$ plot for HII 1554 – HII 1508, showed no strong correlation but the dispersion was in excess expected from the measurement uncertainties, the pattern suggesting that both stars vary in V_i by $\sim 0^m_.03$.

HII 1553 appears redder (listed in J&M) relative to the field stars. From multi-colour photometry by Stauffer (1984), it has been classed as a photometric binary this being confirmed by Bouvier et al. (1997), the companion separated by $0''_.09$.

3.7. Field 7: HII 1776

Summary: B-band 14 frames; V-band 13 frames;
Observations on nights JD 41, JD 42 and JD 46 only;
J&M lists only HII 1776 with B, V values;
4 field stars monitored, 2 with HzC identification.
From the limited run, it was difficult to decipher the behaviour of the monitored stars. Cursory inspection suggested that HII 1776 is variable but not to the degree of HII 1844. On JD 42, this latter star gradually brightened by $\sim 0^m_.1$ relative to both HII 1776 and HII 1900 and may be described as displaying medium level activity.

HII 1844 displayed an anomalous B magnitude (see Fig. 8) possibly as a result of flare activity. HII 1900 is redder in relation to other field stars, lying above the general trend of

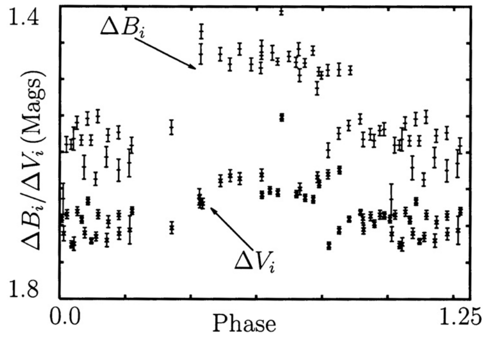

Fig. 7. The ΔB_i, ΔV_i light-curves of HII 3197 based on a period of $0\overset{\mathrm{d}}{.}901$ using values from HII 3167 –#7.

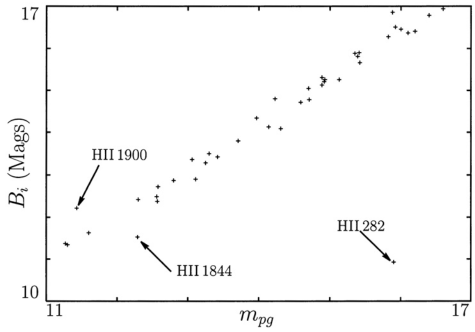

Fig. 8. The correlation between the $m_{\rm pg}$ values in HzC with the B_i magnitudes determined by CCD photometry is very marked. Three labelled stars have anomalous values (see text).

the main sequence (see Fig. 9), and is probably a photometric binary.

3.8. Field 8: HII 3197

Summary: B-band 55 frames; V-band 55 frames;
Observations on JD 41, JD 42, JD 44, JD 46 and JD 47;
J&M lists only HII 3197 with B, V values;
4 field stars monitored, 2 with HzC identification;
#7 used as stable reference.

The stars labelled #6 and #7 exhibited no detectable variability. Surprisingly, no variability was detected for HII 3197 above the measurement noise. Any variability was less than $\sim 0\overset{\mathrm{m}}{.}03$. Krishnamurthi et al. (1998) give a period of $0\overset{\mathrm{d}}{.}44$ with amplitude $\sim 0\overset{\mathrm{m}}{.}03$. From the distribution of ΔB_i, ΔV_i values based on HII 3197 – #7, period detection was not expected, this proving to be the case.

HII 3167 was the most active of stars in the field. The ΔB_i, ΔV_i plot revealed variability of $\sim 0\overset{\mathrm{m}}{.}25$ and $\sim 0\overset{\mathrm{m}}{.}15$ in the respective bands. A suggested period of $0\overset{\mathrm{d}}{.}901$ emerged, although one at $\sim 1\overset{\mathrm{d}}{.}4$ was also possible. Based on the former, the phased data are displayed in Fig. 7, the amplitude for ΔB_i being greater than for ΔV_i. Further data are required to confirm the period. HII 3198 also displayed variability with a range $\sim 0\overset{\mathrm{m}}{.}08$.

The colour index for HII 3197 listed in J&M is anomalous relative to the other field stars. Stauffer (1984) has classed it as a photometric binary; Bouvier et al. (1997) have resolved the system as being triple.

4. Summary discussion

Although the $m_{\rm pg}$ passband in HzC does not match the CCD B-band, the effective wavelengths are fairly close. An excellent correlation between $m_{\rm pg}$ values and the B_i magnitudes, as listed in Table 1, is displayed in Fig. 8, so confirming the data quality presented in this exercise. The systems are related essentially by a linear transformation. Three stars which might be considered as deviants from the correlation are highlighted, their peculiarities being discussed earlier. The extreme departure of HII 282 from the $m_{\rm pg}/B_i$ correlation requires further investigation.

From the $(B_i - V_i)$, V_i values, Fig. 9 presents a raw colour–magnitude diagram, without attempts to correct for interstellar

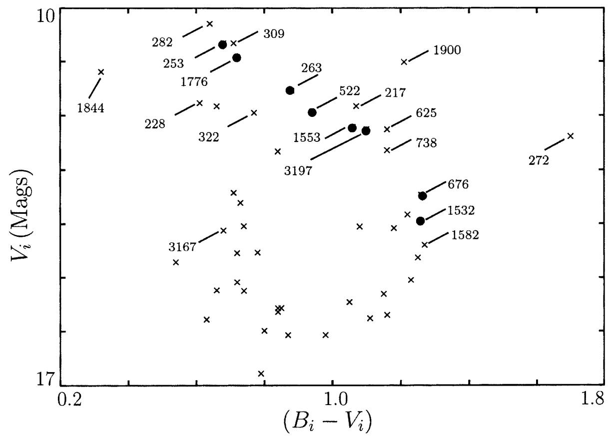

Fig. 9. The HR diagram based on raw $V_i/(B_i - V_i)$ measurements covering solar-type Pleiads. The 8 target stars selected to investigate the $A_{\rm Li}$/surface activity connection are highlighted with heavy dots and form an extension of the main sequence of the brighter stars in the cluster. The enigmatic spread of the HR diagram is very apparent, with a few stars (HII 1990 and HII 272) above the main sequence, suggesting unresolved duplicity, but with many fainter stars below the sequence trend. Other assigned numbers correspond to stars with noted variability. Non-numbered stars appear photometrically quiet, but because of their faintness and poorer measurement accuracies, this generalisation may be imperfect.

extinction, this generally being very small (see Crawford & Perry 1976). The diagram reveals the trend of the target stars, following a smooth extension of the cluster main sequence. Inspection shows two stars (HII 1900 and HII 272) well above this line. The enigmatic spread below the main sequence trend is very apparent. At $(B_i - V_i) = +0.8$, the apparent luminosity covers ~5 mag. Such dispersion cannot result from large variations of interstellar extinction from star to star; simple consideration of the vector rule that $A_V \approx 3E(B-V)$ does not resolve the problem. Although some parts of the cluster are contaminated by interstellar extinction, the effects are far too small to provide the explanation.

Two monitored stars (HII 282 and HII 522) appear to display fadings superimposed on the rotational modulation of photospheric disturbances. Their positions in the colour/brightness diagram suggests they might be photometric binaries. One explanation of the fading behaviour is that they are short-period eclipsing binaries with a dwarf companion. The signature is also similar in character to the behaviour of HAEBE stars. For the latter, the consensus model is based on orbiting disk-like structures with irregularities in dust densities. If they do possess circumstellar dust, any extinction must be fairly neutral. To reiterate, HII 282 certainly deserves follow-up studies with multi-colour photometry and polarimetry.

Four stars have had periods assigned in Table 1. The value of $0\overset{d}{.}777$ for HII 1532 is in excellent agreement with a previous determination by Krishnamurthi et al. (1998). For the other stars, the periods are tentative and further observations are desirable to confirm their values.

Finally, in respect of the purpose of this study, of the nine stars with catalogued $A_{\rm Li}$ measures, comparison with their observed V_i variation, confirms that there is a relation, although there are deviants degrading the correlation. The star with by far the largest variability of the monitored sample (HII 676), was not expected to be all that active from its $A_{\rm Li}$ value. Also HII 3197 provides an anomalous result. According to its value of $A_{\rm Li}$, it would have been expected to display photometric changes $\sim 0\overset{m}{.}2$, whereas any activity was at least a factor of 10 smaller. Other factors affecting the $A_{\rm Li}$ values of individual stars must therefore be present. One fact is inescapable, however; the majority of solar-type stars in the cluster display photometric variability with brightness changes of $0\overset{m}{.}01$ or larger, representing the effects of the rotational modulation of photospheric disturbances. Their activity suggests that, with a good programme of high quality photometry, extension of the data base for measured periods of Pleiads should be guaranteed.

Acknowledgements. ECM was supported as a summer student by the Department of Physics and Astronomy of the University of Glasgow and SO received maintenance as a PPARC research student.

References

Bibo, E. A., & Thé, P. S. 1991, A&AS, 89, 319
Bouvier, J., Rigaut, F., & Nadeau, D. 1997, A&A, 323, 139
Breger, M. 1986, ApJ, 309, 311
Butler, R. P., Cohen, R. D., Duncan, D. K., & Marcy, G. W. 1987, ApJ, 319, L19
Clarke, D. 2002, A&A, 386, 763
Crawford, D. L., & Perry, C. L. 1976, AJ, 81, 419
Duncan, D. K., & Jones, B. F. 1983, ApJ, 271, 663
Hertzsprung, E. 1947, Ann Sterrewacht Leiden, 19, 1A
Jeffries, R. D. 1999, MNRAS, 309, 189
Johnson, H. L., & Mitchell, R. I. 1958, ApJ, 128, 31
Jones, B. F., Shetrone, M., Fischer, D., & Soderblom, D. R. 1996, AJ, 112, 186
King, J. R., Krishnamurthi, A., & Pinsonneault, M. H. 2000, AJ, 119, 859
Krishnamurthi, A., Terndrup, D. M., Pinsonneault, M. H., et al. 1998, ApJ, 493, 914
Magnitskii, A. K. 1987, Sov. Astron., 31, 696
Magnitskii, A. K. 1987, Sov. Astron. Lett., 13, 451
Marilli, E., Catalano, S., & Frasca, A. 1997, Mem. Soc. Astron. Ital., 68, 895
Messina, S., Rodonò, M., & Guinan, E. F. 2001, A&A, 366, 215
O'Dell, M.A., Panagi, P., Hendry, M.A., & Collier Cameron, A. 1995, A&A, 294, 715
Panov, K. P., & Geyer, E. H. 1991, A&A, 242, 112
Rostopchina, A. N., Grinin, V. P., & Okazaki, A., et al. 1997, A&A, 327, 145
Soderblom, D. R., Jones, B. F., & Balachandran, S., et al. 1993, AJ, 106, 1059
Soderblom, D. R., Stauffer, J. R., Hudon, J. D., & Jones, B. F. 1993, ApJS, 85, 315
Stauffer, J. L. 1984, ApJ, 280, 189
Stauffer, J. R., Hartmann, L., Soderblom, D. R., & Burnham, N. 1984, ApJ, 280, 202
Stauffer, J. R., & Hartmann, L. W. 1987, ApJ, 294, 715
van Leeuwen, & F., Alphenaar, P. 1982, The Messenger, 28, 15
van Leeuwen, F., Alphenaar, P., & Meys, J. M. M. 1987, A&AS, 67, 483